DERIVING ANALYTICAL AXISYMMETRIC CROSS SECTION ANALYSIS AND COMPARING WITH FEM SIMULATIONS

Magnus Komperød*
Technological Analyses Centre
Nexans Norway AS
P. O. Box 42, 1751 HALDEN
Norway

ABSTRACT

Direct electrical heating (DEH) is a technology for preventing hydrate formation and wax deposit inside oil and gas pipelines. Nexans Norway AS is researching and developing deep-water DEH solutions. The company has already produced a deep-water DEH piggyback cable that can carry its own weight at 1 070 m water depth. When this DEH system is installed outside the coast of Africa, it will be the world's deepest DEH system.

This paper derives axisymmetric cross section analysis calculations. The calculations are then applied to the deep-water DEH piggyback cable and compared to finite element method (FEM) simulations of the same cable. There are very good agreements between the analytical calculations and the FEM simulations. For three of five analysis results the differences are 0.6% or less. The largest difference is 4.2%, while the average difference (absolute values) is 1.8%.

Keywords: Axial Stiffness; Axisymmetric Analysis; Cross Section Analysis; DEH; Direct Electrical Heating; Offshore Technology; Subsea Cable; Torsion Stiffness.

NOTATION

A	Cross section area of cable element [m^2].
E	E-modulus of cable element [Pa].
$\vec{F}_c$	Load vector of the cable.
$\vec{F}_i$	Load vector of cable element i.
G	G-modulus (shear modulus) of cable element [Pa].
K_c	Stiffness matrix of the cable.
K_i	Stiffness matrix of cable element i.
L	Pitch length of cable element [m].
l	Length of cable element over one pitch length [m].
$M_{T,c}$	The cable's torsion moment [Nm].
$M_{T,i}$	Contribution to the cable's torsion moment from cable element i [Nm].
R	Pitch radius of cable element [m].
r	Element radius of cable element [m].
r_i	Inner element radius of cable element [m].
r_o	Outer element radius of cable element [m].
T_c	The cable's axial tension [N].
T_i	Contribution to the cable's axial tension from cable element i [N].
$\vec{u}_c$	Displacement vector of the cable and all cable elements.
V	Volume of cable element [m^3].
α	Pitch angle of cable element [rad].
ε_c	Axial cable strain [-].
ε_{xx}	Axial element strain [-].
$\gamma_{x\theta}$	Shear strain in hoop direction on the surface perpendicular to the cylinder's axis (length direction) [-].
φ_c	Cable twist per cable unit length [rad/m].
θ	Angular position relative to the center of the cable element [rad].
Π	Potential energy of cable element [J].

Negative values of L indicate left lay direction, and

*Corresponding author: Phone: +47 69 17 35 39 E-mail: magnus.komperod@nexans.com

positive values of L indicate right lay direction. Similarly, negative values of α indicate left lay direction, and positive values of α indicate right lay direction. All other length values are always positive.

INTRODUCTION

The world's increasing energy demand, combined with the exhaustion of many easily accessible oil and gas reserves, drives the petroleum industry into deeper waters. Manufacturers of subsea cables and umbilicals are among those who face the technological challenges of increased water depths.

Another significant challenge of offshore petroleum production is that the pipeline content is cooled by the surrounding water. As the pipeline content drops to a certain temperature, hydrates may be formed and wax may start to deposit inside the pipeline wall. Hydrates and wax may partially, or even fully, block the pipeline. Hydrate formation may start at temperature as high as 25°C, while wax deposit may start at 35-40°C [1].

There are several ways to prevent hydrate formation and wax deposition. An intuitive solution is to apply thermal insulation at the outer surface of the pipeline. However, at long pipelines, low flow rates, or production shut downs, this solution may be insufficient.

Depressurizing the pipeline content may be used to prevent hydrate formation. However, at deep-water pipelines, high pressure is required to bring the pipeline content to topside. Plug removal by depressurizing also faces the same problem at deep-water pipelines [2].

When thermal insulation and depressurizing are insufficient, a commonly used approach is to add chemicals to the pipeline in order to reduce the critical temperature for hydrate formation and wax deposition. Methanol or glycol is commonly used [1, 3]. However, as explained in reference [1], adding chemicals has practical as well as environmental disadvantages.

Another approach to prevent hydrate formation and wax deposition is to use power cables inside the thermal insulation of the pipeline. The power cables function as heating elements heating the pipeline. However, embedding the cables inside the thermal insulation may lead to practical difficulties [1].

A technology that has emerged over the last years is direct electrical heating (DEH). The first DEH system was installed at Statoil's Åsgard oil and gas field in the Norwegian Sea in year 2000 [4]. Nexans Norway AS qualified the DEH technology together with Statoil and SINTEF.

In DEH systems, the electrical resistance of the steel in the pipeline wall is used as a heating element. A single phase cable, referred to as piggyback cable (PBC), is strapped to the pipeline. In the far end (the end of the pipeline far away from the topside) the PBC is connected ("short circuited") to the pipeline. In the near end (the end of the pipeline close to the topside), a two-phase DEH riser cable is connected to the PBC and the pipeline; one phase of the riser cable is connected to the PBC, and the other phase of the riser cable is connected to the pipeline. When the riser cable is energized topside, energy is transferred through the PBC into the steel of the pipeline wall.

Nexans Norway AS is currently developing deep-water DEH solutions. A piggyback cable that is reparable, i.e. can carry its own weight, at 1 070 m water depth is already produced by Nexans in a delivery project. The cross section of this cable is shown in Figure 1. When this DEH system is installed outside the coast of Africa, it will be the world's deepest DEH system [4].

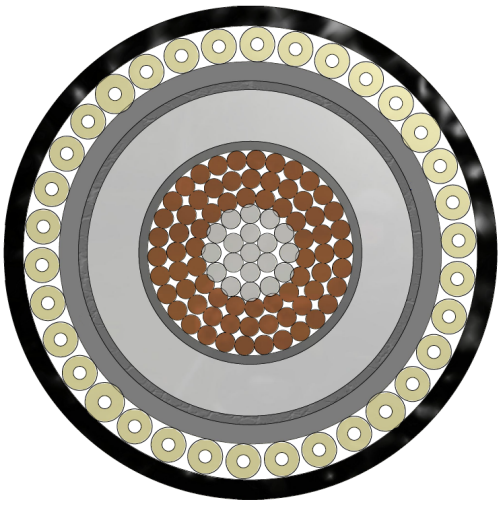

Figure 1: Cross section of the deep-water DEH piggyback cable.

The piggyback cable shown in Figure 1 has 19 (1 + 6 + 12) steel strands in center (gray color in the figure). The purpose of the steel strands is to improve the mechanical capacity of the conductor. This solution is patented by Nexans Norway AS. Outside the steel strands there are 72 (18 + 24 + 30) cop-

per strands (brown color). Outside the stranded conductor there are an electric insulation system (dark gray and light gray colors) and an inner sheath (gray color). Outside the inner sheath there are fillers for mechanical protection (yellow color), and then the outer sheath (black color).
The contribution of this paper is to derive analytical calculations for axisymmetric analysis of the deepwater DEH piggyback cable presented in Figure 1, and compare these analysis results with finite element method (FEM) simulations of the same cable. Analytical calculations increase the analysts' theoretical and practical understanding compared to using FEM tools. Analytical calculations are also very efficient, both in terms of man-hours and CPU time. The analytical derivations presented in this paper are strongly inspired by references [5] and [6].

CROSS SECTION ANALYSIS AND AXISYMMETRIC ANALYSIS

The term cross section analysis refers to a set of analyses on cables, including umbilicals, that describes the cables' mechanical properties. Nexans Norway AS usually includes the following analyses in cross section analyses of DEH cables and umbilicals:

- Axial stiffness when the cable is free to twist [N].
- Axial stiffness when the cable is prevented from twisting [N].
- Bending stiffness [Nm/(m^{-1})].
- Torsion stiffness [Nm/(rad/m)].
- Torsion angle to axial tension ratio when the cable is free to twist [(rad/m)/N].
- Torsion moment to axial tension ratio when the cable is prevented from twisting [Nm/N].
- Capacity during installation.
- Capacity during operation.

The cable's capacity refers to allowed combinations of axial tension [N] and bending curvature [m^{-1}].
Cross section analyses can be done by analytical calculations or by FEM simulations. Reference [5] gives an excellent introduction to the theoretical fundament for analytical calculations. Several other publications, for example references [6] and [7], also cover parts of this theory.
There also exist commercial available software tools for performing cross section analyses. Both software tools based on analytical calculations and software tools based on FEM simulations are available.
The term axisymmetric analysis refers to a subset of those analyses included in the cross section analysis. Axisymmetric analysis includes exactly those analyses where the cable is straight (not bent):

- Axial stiffness when the cable is free to twist [N].
- Axial stiffness when the cable is prevented from twisting [N].
- Torsion stiffness [Nm/(rad/m)].
- Torsion angle to axial tension ratio when the cable is free to twist [(rad/m)/N].
- Torsion moment to axial tension ratio when the cable is prevented from twisting [Nm/N].

As will be shown in this paper, the analyses included in the axisymmetric analysis are mathematically closely related and can be derived from the same stiffness matrix.

DERIVATION OF AXISYMMETRIC ANALYSIS

The derivation presented in this section is strongly inspired by references [5] and [6]. The following assumptions and simplifications apply: (i) Friction is neglected. This is a common assumption in axisymmetric analysis, see for example reference [7]. (Please note that friction is important in the non-axisymmetric part of the cross section analysis.) (ii) Linear elastic materials are assumed. (iii) Radial displacement is neglected. (iv) The Poisson ratio effect is neglected. (v) Helical elements are modeled as tendons. That is, the elements have axial stiffness in tension and compression, while torsion stiffness and bending stiffness are neglected. Please note that the helical elements' influence on the cable's torsion moment and torsion stiffness is included in the model.

From the author's point of view, assumption (i) is probably correct for axisymmetrical analysis in general. The other assumptions must be used with care. In some cases these assumptions have negligible influence on the analysis results, while in other cases they may introduce significant inaccuracy. As shown later in this paper, the analytical calculations give very good agreements with FEM simulations for the deep-water DEH piggyback cable presented in Figure 1. Hence, the applied assumptions do not significantly deteriorate the accuracy of the calculations.

As seen from Figure 1, the cable elements of the PBC can be divided into two types: (i) Non-helical cylinders. Those are the electric isolation system, the inner sheath, and the outer sheath. (ii) Helical elements. Those are the strands of the conductor, as well as the protection fillers. (The center strand of the conductor is modeled as a helical element with zero pitch radius.)

In the axisymmetric case, i.e. when the cable is straight (not bent), the cable has two degrees of freedom: Axial strain, ε_c, and twist per cable unit length, φ_c. These variables are stacked in a vector to form the displacement vector $\vec{u}_c = [\,\varepsilon_c\,,\,\varphi_c\,]^T$. The corresponding loads are: Axial tension, T_c, and torsion moment, $M_{T,c}$. The load vector is then $\vec{F}_c = [\,T_c\,,\,M_{T,c}\,]^T$. The stiffness matrix, K_c, relates the displacement vector and the load vector

$$\vec{F}_c = K_c\,\vec{u}_c \qquad (1)$$
$$\begin{bmatrix} T_c \\ M_{T,c} \end{bmatrix} = \begin{bmatrix} k_{c,11} & k_{c,12} \\ k_{c,21} & k_{c,22} \end{bmatrix} \begin{bmatrix} \varepsilon_c \\ \varphi_c \end{bmatrix}.$$

As will be explained later in this paper, the displacement vector, $\vec{u}_c$, is common for all cable elements, as well as for the cable itself. The load vectors and the stiffness matrices are individual to each cable element. The load vector of cable element i is $\vec{F}_i$, while the load vector of the cable is $\vec{F}_c$. Similarly, the stiffness matrix of cable element i is K_i, and the stiffness matrix of the cable is K_c. The following text derives the stiffness matrices for cylinder cable elements and for helical cable elements.

Stiffness Matrix of a Cylinder Cable Element

Subject to the degrees of freedom presented above, the potential energy, Π, of a non-helical cylinder over an axial length L can be expressed as

$$\Pi(\varepsilon_c,\varphi_c) = \int_V \left(\frac{1}{2}E{\varepsilon_{xx}}^2 + \frac{1}{2}G{\gamma_{x\theta}}^2\right) \mathrm{d}V \qquad (2)$$
$$- T_i L\varepsilon_c - M_{T,i} L\varphi_c.$$

The last two terms of Eq. 2 are the potential energy of the applied loads. The first expression in the integration term of Eq. 2 is the strain energy in the cylinder due to axial tension. As the cylinder is non-helical, the axial strain of the cylinder, ε_{xx}, is equal to the axial strain of the cable, ε_c. Also, the axial strain is equal over the cylinder volume. This simplifies to

$$\int_V \frac{1}{2}E{\varepsilon_{xx}}^2\,\mathrm{d}V = \frac{1}{2}E{\varepsilon_c}^2 \int_V \mathrm{d}V \qquad (3)$$
$$= \frac{1}{2}E{\varepsilon_c}^2 \int_0^L \int_0^{2\pi} \int_{r_i}^{r_o} r\,\mathrm{d}r\,\mathrm{d}\theta\,\mathrm{d}L$$
$$= \frac{\pi}{2}EL({r_o}^2 - {r_i}^2){\varepsilon_c}^2.$$

The second term in the integration term of Eq. 2 is the strain energy in the cylinder due to torsion. A simple geometric consideration shows that the shear strain, $\gamma_{x\theta}$, is given by $\gamma_{x\theta} = r\varphi_c$. As φ_c is constant over the cable volume, it follows that

$$\int_V \frac{1}{2}G{\gamma_{x\theta}}^2\,\mathrm{d}V = \int_V \frac{1}{2}Gr^2{\varphi_c}^2\,\mathrm{d}V \qquad (4)$$
$$= \frac{1}{2}G{\varphi_c}^2 \int_V r^2\,\mathrm{d}V$$
$$= \frac{1}{2}G{\varphi_c}^2 \int_0^L \int_0^{2\pi} \int_{r_i}^{r_o} r^2\,r\,\mathrm{d}r\,\mathrm{d}\theta\,\mathrm{d}L$$
$$= \frac{\pi}{4}GL({r_o}^4 - {r_i}^4){\varphi_c}^2.$$

Eq. 2 can then be rewritten as

$$\Pi(\varepsilon_c,\varphi_c) = \frac{\pi}{2}EL({r_o}^2 - {r_i}^2){\varepsilon_c}^2 \qquad (5)$$
$$+ \frac{\pi}{4}GL({r_o}^4 - {r_i}^4){\varphi_c}^2$$
$$- T_i L\varepsilon_c - M_{T,i} L\varphi_c.$$

The cable is in equilibrium when the potential energy, Π, is at a stationary point. The equilibrium conditions are then

$$\frac{\partial \Pi(\varepsilon_c, \varphi_c)}{\partial \varepsilon_c} = \pi E L({r_o}^2 - {r_i}^2)\varepsilon_c - T_i L = 0, \quad (6)$$

$$\frac{\partial \Pi(\varepsilon_c, \varphi_c)}{\partial \varphi_c} = \frac{\pi}{2} G L({r_o}^4 - {r_i}^4)\varphi_c - M_{T,i} L = 0. \quad (7)$$

Dividing Eq. 6 and Eq. 7 by L gives

$$T_i = \pi E({r_o}^2 - {r_i}^2)\varepsilon_c, \quad (8)$$

$$M_{T,i} = \frac{\pi}{2} G({r_o}^4 - {r_i}^4)\varphi_c. \quad (9)$$

The stiffness matrix of a cylinder cable element is then given by

$$\vec{F}_i = K_i \vec{u}_c \quad (10)$$

$$\begin{bmatrix} T_i \\ M_{T,i} \end{bmatrix} = \begin{bmatrix} \pi E({r_o}^2 - {r_i}^2) & 0 \\ 0 & \frac{\pi}{2} G({r_o}^4 - {r_i}^4) \end{bmatrix} \begin{bmatrix} \varepsilon_c \\ \varphi_c \end{bmatrix}.$$

Stiffness Matrix of a Helical Cable Element

As stated above, the helical cable elements are modeled as tendons. This means that these elements' bending stiffness and torsion stiffness are neglected. The helical element's potential energy over a pitch length, L, is then

$$\Pi(\varepsilon_c, \varphi_c) = \int_V \frac{1}{2} E {\varepsilon_{xx}}^2 \, \mathrm{d}V - T_i L \varepsilon_c - M_{T,i} L \varphi_c. \quad (11)$$

The last two terms of Eq. 11 are the potential energy of the applied loads. The integration term of Eq. 11 is the strain energy in the helical element due to its axial strain. Because bending stiffness and thereby strain from bending are neglected, the axial strain is equal over the element's volume. Hence, the strain energy can be written as

$$\begin{aligned} \int_V \frac{1}{2} E {\varepsilon_{xx}}^2 \, \mathrm{d}V &= \frac{1}{2} E {\varepsilon_{xx}}^2 \int_V \mathrm{d}V \\ &= \frac{1}{2} E {\varepsilon_{xx}}^2 \int_0^l \int_0^{2\pi} \int_0^r r \, \mathrm{d}r \, \mathrm{d}\theta \, \mathrm{d}l \\ &= \frac{\pi}{2} E l r^2 {\varepsilon_{xx}}^2 \\ &= \frac{1}{2} \frac{EAL}{\cos(\alpha)} {\varepsilon_{xx}}^2 \end{aligned} \quad (12)$$

In the last line of Eq. 12, it is used that $A = \pi r^2$ and $l = L/\cos(\alpha)$. As for the cylinder case, the helical element is in equilibrium when the potential energy, Π, is at a stationary point. Inserting Eq. 12 into Eq. 11 and differentiating gives

$$\frac{\partial \Pi(\varepsilon_c, \varphi_c)}{\partial \varepsilon_c} = \frac{EAL}{\cos(\alpha)} \varepsilon_{xx} \frac{\partial \varepsilon_{xx}}{\partial \varepsilon_c} - T_i L = 0, \quad (13)$$

$$\frac{\partial \Pi(\varepsilon_c, \varphi_c)}{\partial \varphi_c} = \frac{EAL}{\cos(\alpha)} \varepsilon_{xx} \frac{\partial \varepsilon_{xx}}{\partial \varphi_c} - M_{T,i} L = 0. \quad (14)$$

The next issue is to derive ε_{xx} as function of ε_c and φ_c. While helical elements are three dimensional geometries, it is common to illustrate these geometries in two dimensions as shown in Figure 2. The pitch length, L, is the axial length of the cable corresponding to one revolution of the helix. Elements in the same cable layer always have the same pitch length. The element length, l, is the length of the cable element over one pitch length. The pitch radius, R, is the radius from center of the cable to center of the element. The pitch angle, α, is the angle between the cable's axis (length direction) and the tangent of the helix. Figure 2 shows the geometric relation between L, R, θ, l, and α. This relation is true for $\theta = 2\pi$ rad.

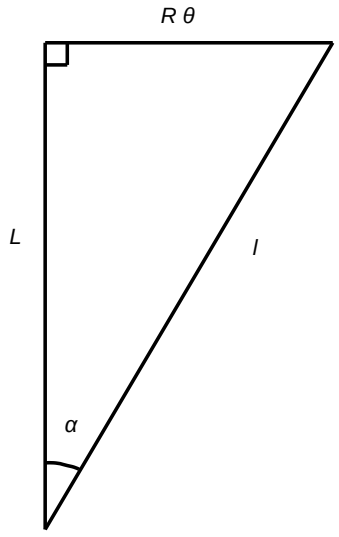

Figure 2: Geometric relation between L, l, R, θ, and α. The relation it true for $\theta = 2\pi$ rad.

Based on Figure 2, Pythagoras' theorem gives

$$l^2 = L^2 + (R\theta)^2. \tag{15}$$

Differentiation of Eq. 15 and division by $2l^2$ gives

$$\frac{\mathrm{d}l}{l} = \frac{L\mathrm{d}L}{l^2} + \frac{R^2\theta\mathrm{d}\theta}{l^2}. \tag{16}$$

In Eq. 16, R is a constant. Inserting $l = L/\cos(\alpha)$, $l = R\theta/\sin(\alpha)$, and $\theta = 2\pi$ rad gives

$$\frac{\mathrm{d}l}{l} = \cos^2(\alpha)\frac{\mathrm{d}L}{L} + \sin^2(\alpha)\frac{\mathrm{d}\theta}{2\pi}, \tag{17}$$

$$\varepsilon_{xx} = \cos^2(\alpha)\varepsilon_c + \sin^2(\alpha)\frac{L}{2\pi}\varphi_c, \tag{18}$$

$$\varepsilon_{xx} = \cos^2(\alpha)\varepsilon_c + R\cos(\alpha)\sin(\alpha)\varphi_c. \tag{19}$$

In Eq. 18 it has been used that $\varepsilon_{xx} \stackrel{\text{def}}{=} \mathrm{d}l/l$, $\varepsilon_c \stackrel{\text{def}}{=} \mathrm{d}L/L$, and $\mathrm{d}\theta = L\varphi_c$. In Eq. 19 it has been used that $\tan(\alpha) = 2\pi R/L$. Inserting Eq. 19 and its partial derivatives into Eq. 13 and Eq. 14, and dividing the latter equations with L gives

$$\begin{aligned} T_i =& EA\cos^3(\alpha)\varepsilon_c \\ &+ EAR\cos^2(\alpha)\sin(\alpha)\varphi_c, \end{aligned} \tag{20}$$

$$\begin{aligned} M_{T,i} =& EAR\cos^2(\alpha)\sin(\alpha)\varepsilon_c \\ &+ EAR^2\cos(\alpha)\sin^2(\alpha)\varphi_c. \end{aligned} \tag{21}$$

The stiffness matrix for helical elements is then

$$\vec{F}_i = K_i\vec{u}_c \tag{22}$$

$$\begin{bmatrix} T_i \\ M_{T,i} \end{bmatrix} = \begin{bmatrix} k_{i,11} & k_{i,12} \\ k_{i,21} & k_{i,22} \end{bmatrix} \begin{bmatrix} \varepsilon_c \\ \varphi_c \end{bmatrix},$$

$$\begin{aligned} k_{i,11} &= EA\cos^3(\alpha), \\ k_{i,12} &= k_{i,21} = EAR\cos^2(\alpha)\sin(\alpha), \\ k_{i,22} &= EAR^2\cos(\alpha)\sin^2(\alpha). \end{aligned}$$

Stiffness Matrix of Cable

The previous sections derive the stiffness matrices of non-helical cylinder elements and helical elements. This section explains how to calculate the stiffness matrix of the cable based on stiffness matrices of the cable elements.

All cable elements, as well as the cable itself, are subject to the same strain along the cable's length direction, ε_c, and the same twist along the cable's axis, φ_c. Hence, they all share the same displacement vector $\vec{u}_c = [\varepsilon_c, \varphi_c]^T$.

The axial tension of the cable, T_c, is equal to the contributions from all cable elements, $\sum_i T_i$. Similarly, the torsion moment of the cable, $M_{T,c}$, is equal to the contributions from all cable elements, $\sum_i M_{T,i}$. Therefore, the cable's load vector is equal to the sum of the load vectors of all cable elements. That is

$$\begin{aligned} \vec{F}_c &= \sum_i \vec{F}_i, \\ K_c\vec{u}_c &= \sum_i K_i\vec{u}_c = \left(\sum_i K_i\right)\vec{u}_c. \end{aligned} \tag{23}$$

Comparison in the second row of Eq. 23 proves that the stiffness matrix of the cable, K_c, is equal to the sum of the stiffness matrices of all cable elements, i.e.

$$K_c = \sum_i K_i. \tag{24}$$

Computing Axisymmetric Analysis Results

The previous section shows how to compute the cable's stiffness matrix. This section explains how to compute the axisymmetric analysis results from the stiffness matrix. The stiffness matrix is on the form

$$\begin{bmatrix} T_c \\ M_{T,c} \end{bmatrix} = \begin{bmatrix} k_{c,11} & k_{c,12} \\ k_{c,21} & k_{c,22} \end{bmatrix} \begin{bmatrix} \varepsilon_c \\ \varphi_c \end{bmatrix}. \tag{25}$$

Note that $k_{c,12} = k_{c,21}$, both for non-helical cylinders, for helical elements, and hence for the cable itself. It is in this context more convenient to write the matrix as a set of linear equations, where it is used that $k_{c,12} = k_{c,21}$. That is

$$T_c = k_{c,11}\varepsilon_c + k_{c,12}\varphi_c, \tag{26}$$

$$M_{T,c} = k_{c,12}\varepsilon_c + k_{c,22}\varphi_c. \tag{27}$$

The following sections derive the axisymmetric results. Please note that the stiffness matrix of the cable must be calculated first, using Eq. 24, and then be

used in the calculations presented below. The opposite, i.e. to first compute the axisymmetric analyses for each cable element, and then sum these analyses to obtain the analysis for the cable will give erroneous results (except for in some special cases).

Axial Stiffness at Free Twist

When the cable is free to twist, it does not set up any torsion moment. Inserting $M_{T,c} = 0$ into Eq. 27, solving for φ_c, and inserting this into Eq. 26 gives

$$T_c = \left(k_{c,11} - \frac{{k_{c,12}}^2}{k_{c,22}} \right) \varepsilon_c. \tag{28}$$

Hence, the axial stiffness at free twist is $k_{c,11} - \frac{{k_{c,12}}^2}{k_{c,22}}$.

Axial Stiffness at No Twist

No twist is equivalent to $\varphi_c = 0$. Inserting this into Eq. 26 gives $T_c = k_{c,11}\varepsilon_c$. Hence, the axial stiffness at no twist is $k_{c,11}$.

Torsion Stiffness at Free Elongation

Solving Eq. 26 for ε_c and inserting this into Eq. 27 gives

$$M_{T,c}(T_c, \varphi_c) = \frac{k_{c,12}}{k_{c,11}} T_c + \left(k_{c,22} - \frac{{k_{c,12}}^2}{k_{c,11}} \right) \varphi_c, \tag{29}$$

$$\frac{\partial M_{T,c}(T_c, \varphi_c)}{\partial \varphi_c} = k_{c,22} - \frac{{k_{c,12}}^2}{k_{c,11}}. \tag{30}$$

Hence, the torsion stiffness at free elongation is $k_{c,22} - \frac{{k_{c,12}}^2}{k_{c,11}}$. Please note that in Eq. 29 and Eq. 30, $M_{T,c}$ is a function of T_c and φ_c, not a function of ε_c as in the other cases.

Torsion Angle to Axial Tension Ratio

In this case, the cable is free to twist, i.e. it sets up no torsion moment. Inserting $M_{T,c} = 0$ into Eq. 27, solving for ε_c, and inserting this into Eq. 26 gives

$$T_c = \left(-\frac{k_{c,11}k_{c,22}}{k_{c,12}} + k_{c,12} \right) \varphi_c, \tag{31}$$

$$\frac{\varphi_c}{T_c} = \frac{k_{c,12}}{{k_{c,12}}^2 - k_{c,11}k_{c,22}}. \tag{32}$$

Hence, the torsion angle to axial tension ratio is $\frac{k_{c,12}}{{k_{c,12}}^2 - k_{c,11}k_{c,22}}$.

Torsion Moment to Axial Tension Ratio

In this case, the cable is prevented from twisting. Inserting $\varphi_c = 0$ into Eq. 26 and Eq. 27, and solving both equations for ε_c gives

$$\varepsilon_c = \frac{T_c}{k_{c,11}} = \frac{M_{T,c}}{k_{c,12}}, \tag{33}$$

$$\frac{M_{T,c}}{T_c} = \frac{k_{c,12}}{k_{c,11}}. \tag{34}$$

Hence, the torsion moment to axial tension ratio is $\frac{k_{c,12}}{k_{c,11}}$.

UFLEX2D

The UFLEX program system originates from a joint Marintek and Nexans effort kicked off in 1999, resulting in a 2D software module (UFLEX2D) for structural analysis of complex umbilical cross-sections. The first version of the tool was launched in 2001. From 2005 and onwards further development of the 2D module as well as the development of a 3D module (UFLEX3D) has taken place within a Joint Industry Project (JIP). The JIP is still running, and is financed by a group of 10 sponsors covering the following oil and gas industry segments; operators, suppliers, technical service providers.

UFLEX2D is a finite element method (FEM) tool, which can be used to simulate all analysis results that Nexans Norway AS includes in cross section analyses. Figure 3 shows the UFLEX2D FEM model of the deep-water DEH piggyback cable presented in Figure 1.

COMPARING ANALYTICAL CALCULATIONS WITH FEM SIMULATIONS

Table 1 presents the differences of the analytical calculations derived in this paper and the results of the UFLEX2D FEM simulations. The table shows that there are very good agreements between the analytical calculations and the FEM simulations. For three of the five results the differences are 0.6% or less. The largest difference is 4.2%. The average difference (absolute values) is 1.8%.

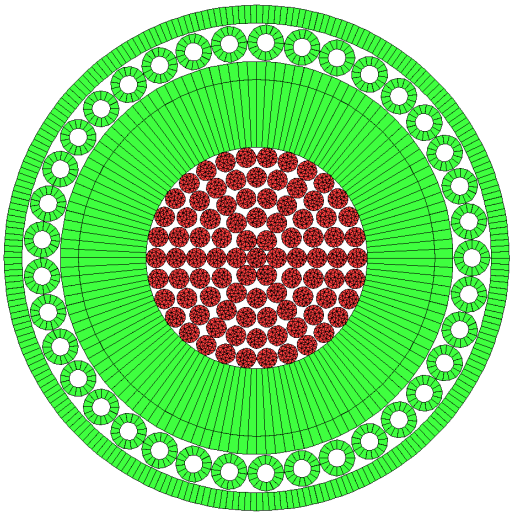

Figure 3: Finite element model of the deep-water DEH piggyback cable. The colors of the figure do not represent any physical values.

Analysis Result	**Difference** [%]
Axial stiffness (free twist)	0.6
Axial stiffness (no twist)	0.3
Torsion stiffness (free elongation)	−3.8
Torsion angle to axial tension ratio	4.2
Torsion moment to axial tension ratio	0.0

Table 1: Differences between analytical calculations and UFLEX2D FEM simulations.

Based on the good agreements between the analytical calculations and the FEM simulations, it is concluded that the analytical derivations presented in this paper cover the significant physical effects of the deep-water DEH piggyback cable. Further it is concluded that the applied assumptions and simplifications do not significantly deteriorate the accuracy of the calculations.

CONCLUSIONS

This paper derives analytical calculations for axisymmetric analyses. These calculations have been used to compute the axisymmetric analysis results for a deep-water DEH piggyback cable developed by Nexans Norway AS. This piggyback cable is reparable, i.e. can carry its own weight, at 1 070 m water depth. The development of the piggyback cable is part of Nexans' efforts towards deep-water DEH solutions.

The analytical calculations are compared to UFLEX2D FEM simulations. There are very good agreements between the analytical calculations and the FEM simulations. For three of the five analysis results the differences are 0.6% or less. The largest difference is 4.2%, while the average difference (absolute values) is 1.8%.

REFERENCES

[1] A. Nysveen, H. Kulbotten, J. K. Lervik, A. H. Børnes, M. Høyer-Hansen, and J. J. Bremnes. Direct Electrical Heating of Subsea Pipelines - Technology Development and Operating Experience. *IEEE Transactions on Industry Applications*, 43:118 – 129, 2007.

[2] J. K. Lervik, M. Høyer-Hansen, Ø. Iversen, and S. Nilsson. New Developments of Direct Electrical Heating for Flow Assurance. In *Proceedings of the Twenty-second (2012) International Offshore and Polar Engineering Conference - Rhodes, Greece*, 2012.

[3] S. Dretvik and A. H. Børnes. Direct Heated Flowlines in the Åsgard Field. In *Proceedings of the Eleventh (2001) International Offshore and Polar Engineering Conference - Stavanger, Norway*, 2001.

[4] S. Kvande. Direct Electrical Heating Goes Deeper. *E&P Magazine June 2014*, 2014.

[5] E. Kebadze. *Theoretical Modelling of Unbonded Flexible Pipe Cross-Sections*. PhD thesis, South Bank University, 2000.

[6] R. H. Knapp. Derivation of a new stiffness matrix for helically armoured cables considering tension and torsion. *International Journal for Numerical Methods in Engineering*, 14:515 – 529, 1979.

[7] N. Sødahl, G. Skeie, O. Steinkjær, and A. J. Kalleklev. Efficient fatigue analysis of helix elements in umbilicals and flexible risers. In *Proceedings of the ASME 29th International Conference on Ocean, Offshore and Arctic Engineering OMAE 2010*, 2010.